J Mater Sci (2007) 42:3816–3824
DOI 10.1007/s10853-006-0408-x

Electrical conductivity studies of $AgI–Ag_2O–B_2O_3–TeO_2$ glasses

V. C. Veeranna Gowda · R. V. Anavekar

Received: 17 March 2005 / Accepted: 5 May 2006 / Published online: 12 February 2007

Abstract The silver ion conducting boro tellurite glasses have been prepared by melt quenching technique. The conductivity and dielectric measurements were carried out on these glasses as a function of frequency from 10 Hz to 10 MHz over a temperature range of 298–328 K. The analysis of conductivity measurement shows that the silver ions are the main charge carriers, which are considered to be the predominant factor playing the role of enhancing the conductivity. The power law exponent s and stretched exponent β are found to be insensitive to both temperature and compositions. AC conductivity and dielectric relaxation behaviour of these glasses were also studied and the results are discussed in view of the structure of borate and tellurite network.

Introduction

Superionic conducting glassy materials are of technological interest from the point of view of their potential usage as solid electrolyte in the fabrication of solid state batteries. Several electrical studies on glassy materials have revealed that glasses need not necessarily be insulators, but can be superionic conductors under certain circumstances [1–3]. The high ionic conductivity depends on the nature and content of the modifier oxide and also glass former compositions [4, 5]. The incorporation of alkali halides or metal halides in the mixed glass formers [6, 7] is considered to be predominant factor playing the role of enhancing the conductivity of the conventional glasses to reach the values of superionic materials. The fast ion conducting glasses are characterized by greater freedom of movement of Ag^+/Li^+ ions because these ions are not held in the lattice sites or anion cages firmly. Also the addition of network modifier such as Ag_2O introduces ionic bonds usually associating non-bridging oxygen ions with modifying cations. Ag_2O donates oxygens and negative charges to the glass network, which becomes rich in charge carriers (Ag^+) and gains the capability of acting as a solvent for the metal halide (AgI) salts. Hence the mobility of Ag^+ ions associated with an iodide environment is considered to be higher and based on the fact that increase in the percentage of AgI in the glass give rise to higher conductivities [8–10].

One of the most widely used glass formers for the synthesis of superionic conducting glass is B_2O_3. Generally glasses containing silver halide and particularly silver iodide, can provide superionic behaviour at room temperature. The structure and the electrical properties of silver ion-conducting borate-based glasses have been reported in the literature [11, 12]. Borate glasses exhibit well-known and unique structural features. The glass structure consist of three coordinated trigonal $[BO_{3/2}]^0$ and four connected tetrahedral $[BO_{4/2}]^-$ boron atoms and these $[BO_{4/2}]^-$ atoms are produced by the modification at the expense of $[BO_{3/2}]^0$ units [13, 14]. The trigonal and tetragonal conversion and formation of oxygen bridges by the oxide ion from the modifier reaches a maximum at the diborate composition. When the modifier concentration is increased further, the percentage of

V. C. V. Gowda · R. V. Anavekar (✉)
Department of Physics, Bangalore University,
Bangalore 560 056, India
e-mail: anavekar_271@yahoo.co.in

tetragonal boron decreases indicating a structural stability of tetrahedra in the presence of higher modifier oxide concentrations [15–18] and the notable feature is that there is no non-bridging oxygen (NBO) in the coordination of tetrahedral boron. Tellurium oxide is also a good network former and a large number of binary and ternary tellurite systems easily form glasses [19, 20]. The structure of tellurite glasses has been examined by many authors [21–23] using various techniques. The interesting aspect of the structure of tellurite glasses is that when the environment is more ionic, the addition of modifier seems to favour the formation of trigonal pyramidal, $[TeO_{3/2}]^{-}$ (tp) units at the expense of trigonal bipyramidal, $[TeO_{4/2}]^{0}$ (tbp) units [24–29]. Tellurium appears to prefer these coordinations, tp units form chains while tbp units show three dimensional networks. Also when TeO_2 is added to the borate group (such as diborate) which is quite ionic, TeO_2 prefers to form chains which interpenetrate the borate network. Tellurium oxide-based glasses are mainly studied for their optical properties. The investigations of electrical conductivity from AgI–Ag_2O–TeO_2 glass system have been studied recently. Due to a lone electronic pair associated with tellurium leads to high refractive index [21] and show interesting non-linear optical transmission in the infrared region [30, 31]. They also exhibit high dielectric constant and ionic conductivity with suitable modifications of the network [29, 32, 33]. In addition to all these properties, tellurite glasses exhibit low glass transition temperature, high thermal expansion coefficient and are less hygroscopic in nature (compared to phosphate and other oxide glasses), which make them responsible for their applications in optical switching devices, erasable recording materials, laser hosts etc. [34–37].

It has been observed that in many cases the conductivities have been enhanced by mixing two different glass formers [8, 9, 38–40] with different coordination polyhedrons. But such mixtures have a strong tendency to phase separation at low modifier oxide molar ratio. Therefore, the complete substitution of one network former by another one has not always been possible [9].

The present study, aims to investigate the glasses containing two glass formers (B_2O_3 and TeO_2) by replacing high conducting electrolyte material such as AgI by Ag_2O. Silver oxides has been chosen as a network modifying oxide, since silver ions possess high ionic conductivity compared to alkali modifying cations such as Li^+ ion. Keeping a constant molecular ratio of the network former, an increase of the ionic conductivity has been observed by mixing two different network modifiers. The frequency dependence of conductivity and dielectric relaxation has also been examined.

Experimental

Glasses in the quaternary system, AgI–Ag_2O–B_2O_3–TeO_2 are prepared using high purity chemicals, AgI (Qualigens), Ag_2O (Qualigens), H_3BO_3 (BDH) and TeO_2 (Aldrich). The ratio between B_2O_3 and TeO_2 is kept constant, (B_2O_3:$TeO_2 = 1$) and AgI content is varied between 0 and 12.5 mol%. The glass samples were prepared by melting the calculated quantities of analar grade chemicals in porcelain crucibles. The mixtures were melted in an electric furnace in the temperature range of 900–950 °C depending on composition. The melted liquid being mixed by swirling the melt to obtain a bubble-free and homogeneous glass. The melt was poured on to a brass block and pressed with another block to obtain thin discs of 0.1 cm thickness and a diameter of 1 cm. The obtained glassy samples were then annealed at a temperature lower than the glass transition temperature in order to remove the internal stresses. All the glasses were checked for amorphous nature by X-ray diffractograms, which did not show any sharp peaks.

Electrical conductivity measurements were carried out on a Hewlett Packard HP 4192 A impedance-gain phase analyzer from 10 Hz to 10 MHz in the temperature range of 298–328 K. A home-built cell assembly (a two-terminal capacitor configuration and spring loaded electrodes of silver) was used for the measurements. The sample temperature was measured using a Pt-Rh thermocouple positioned very close to the sample. The temperature was controlled using a Heatcon (Bangalore, India) temperature controller and the temperature constancy of ±1 K was achieved in the entire range of measurements. Annealed circular glass pieces, coated with silver paint on both sides and having thickness of about 0.1 cm and a diameter of 1 cm were used for the measurements.

Analysis procedure

The capacitance (C_p) and conductance (G) of all the samples were measured from the impedance analyser. These were used to evaluate the real and imaginary parts of the complex impedance using standard relations

$$Z^* = Z' + jZ'' = \frac{1}{(G + j\omega C_p)} \qquad (1)$$

$$Z' = \frac{G}{(G^2 + \omega^2 C_{\mathrm{p}}^2)} \tag{2}$$

$$Z'' = \frac{\omega C_{\mathrm{p}}}{(G^2 + \omega^2 C_{\mathrm{p}}^2)} \tag{3}$$

The dc conductances were determined from the semicircular complex impedance (Z' versus Z'') plots by taking the value of intersection of the low frequency end of the semicircle on Z' axis. The conductivity (σ) for each sample was calculated using the expression

$$\sigma = G\left(\frac{d}{A}\right) \tag{4}$$

where d and A are the thickness and area of the sample, respectively.

The real (ε') and imaginary (ε'') parts of the complex dielectric constant were calculated from the relations,

$$\varepsilon' = \frac{C_{\mathrm{p}} d}{A \varepsilon_0} \tag{5}$$

$$\varepsilon'' = \frac{\sigma}{\varepsilon_0 \omega} \tag{6}$$

where ε_0 is the permittivity of the free space.

The data were also analysed using the electrical modulus formalism. The real (M') and imaginary (M'') parts of the complex electrical modulus ($M^* = 1/\varepsilon^*$) were obtained from ε' and ε'' values using the relations,

$$M' = \frac{\varepsilon'}{(\varepsilon'^2 + \varepsilon''^2)} \tag{7}$$

$$M'' = \frac{\varepsilon''}{(\varepsilon'^2 + \varepsilon''^2)} \tag{8}$$

Results and discussion

DC conductivity

The compositions of the glasses investigated in this study are given in Table 1 along with their corresponding codes. The typical impedance plots (Cole–Cole plots) for BT2 glass is shown in Fig. 1 for four different temperatures.

The dc conductivities were determined from impedance plots from the intercepts on the real axis (Z') corresponding to zero frequency. The intercept point shifted to lower and lower Z' values with increase of temperature. The Arrhenius plots of conductivities (σ_{dc}) for all the glasses are shown in Fig. 2. The behaviour of dc conductivities of all the glasses is found to be similar.

As can be seen from Fig. 2 that the conductivity gradually increases with increase of AgI mol% although, the concentration of Ag^+ ion has been maintained constant in all the compositions. The increasing trend in conductivity with AgI concentration is due to the fact that the incorporation of metal halides was considered as the predominant factor playing the role of enhancing the conductivity [4, 7]. In order to examine the influence of metal halide, AgI itself on the observed conductivity, log σ_{dc} has been re-plotted as a function of AgI mol% and it is shown in Fig. 3. The conductivity progressively increases with increase of AgI mol%. In silver boro tellurite glasses, both TeO_2 and B_2O_3 compete each other for the oxygen available from the modifier Ag_2O and consequently the oxygens supplied from Ag_2O is utilized by TeO_2. This expectation is favored by considering its electronegativities. Since the molecular electronegativities [41] of $[BO_{3/2}]^0$ = 2.79 and that of $[TeO_{4/2}]^0$ = 2.95 [41]. Therefore, the added oxygens supplied by Ag_2O are utilized by TeO_2 and it is well known that Te in TeO_2 glass is coordinated by four oxygen atoms to form $[TeO_{4/2}]^0$ tetrahedral units. The four coordination of Te is found to decrease with the addition of modifier oxide [21, 29]. This change in coordination is considered to be due to the ability of modifier oxide to break some of Te–O–Te bonds. This would lead to the creation of $[TeO_{3/2}]^-$ units with non-bridging oxygen atoms (NBO's). The addition of modifying oxide leads to increasing the formation of $[TeO_{3/2}]^-$ at the expense of $[TeO_{4/2}]^-$ groups. This would particularly lead to weakening the tellurium cyclic arrangement. This structural rearrangement helps the tellurite network to be able to accommodate the more AgI composition. This also enables the glassy matrix to dissolve the AgI salt. This dissolution of AgI in the tellurium network is considered to be most dominant factor, which is responsible to enhance the conductivity [32, 42–46]. The enhancement of conductivity is also consistent with the model of the glass structure proposed by Minami et al. [47], which considers three types of Ag^+ ions occurs in the glasses. The first are Ag^+ ions bonded with non-bridging oxygen with strong partial covalency, the second are Ag^+ ions surrounded with halide ions (X^-) only, and the third are Ag^+ ions

Table 1 Compositions of the glasses along with codes of designation, room temperature (RT) conductivities, dc and ac activation energies

Code	Composition in mol%				σ (S cm^{-1}) at RT	E_{dc} (eV)	E_{ac} (eV)
	AgI	Ag_2O	B_2O_3	TeO_2			
BT1	0	30	35	35	2.68×10^{-7}	0.52	0.50
BT2	2.5	27.5	35	35	6.28×10^{-7}	0.46	0.43
BT3	5	25	35	35	1.06×10^{-6}	0.44	0.40
BT4	7.5	22.5	35	35	2.34×10^{-6}	0.42	0.37
BT5	10	20	35	35	3.75×10^{-6}	0.36	0.34
BT6	12.5	17.5	35	35	5.26×10^{-6}	0.33	0.30

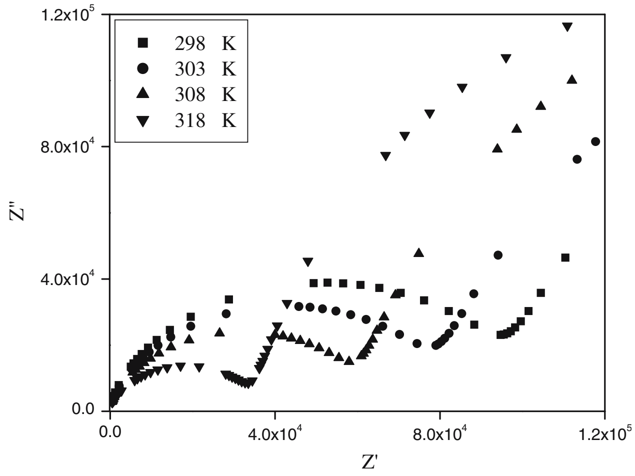

Fig. 1 Typical impedance plots of BT2 glass at different temperatures

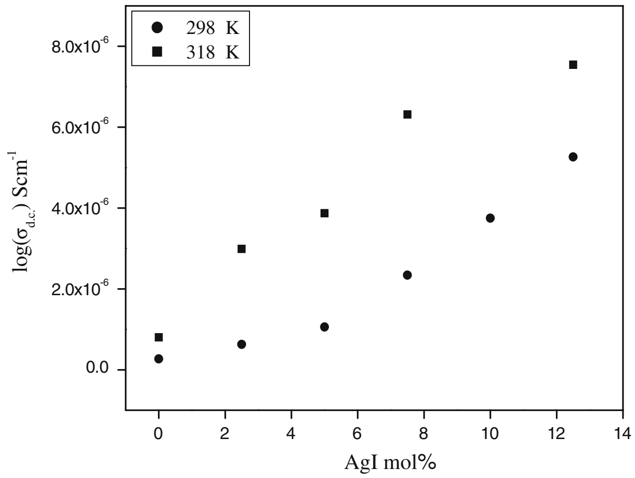

Fig. 3 Variation of log(σ_{dc}) versus AgI mol%

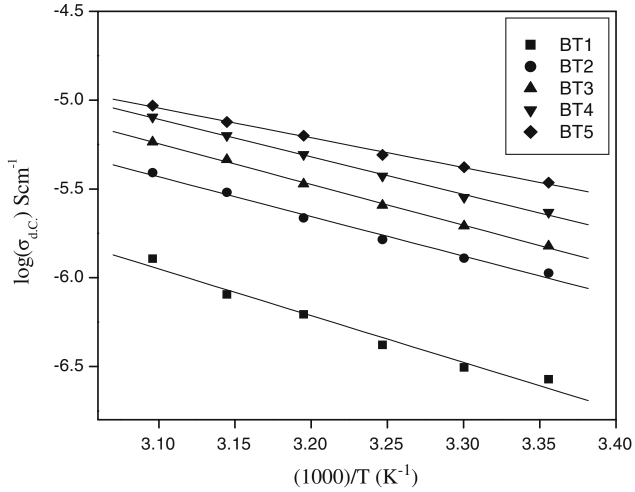

Fig. 2 Variation of log($\sigma_{d.c.}$) versus (1000/T) for all the glass samples

interacting with $[BO_{4/2}]^-$ groups. The experimental results obtained in the present glass system leads to a conclusion that not only Ag^+ ions interact with halide ions but also Ag^+ ions interacting with anions other than halide ions must contribute to the enhancement of conductivity. Since the addition of Ag_2O preserves $[BO_{4/2}]^-$ groups in the glass matrix while on increasing AgI content, the number of $[BO_{4/2}]^-$ groups drastically decreases due to the formation of structural groups with non-bridging oxygens resulting the appearance of distorted $[TeO_{3/2}]^-$ groups. [48].

The data of each sample has been least square fitted to straight line to evaluate the activation energy (with an error ± 0.03) for electrical conduction. The values of dc activation energies (E_{dc}) determined from log(σ_{dc}) versus (1000/T) plots are given in Table 1. The values of E_{dc} have been plotted and their variation as a function of AgI concentration is shown in Fig. 4. The decrease of activation energies complements the observed variation in the conductivity which is due to the degradation of boro-tellurite network.

AC conductivity

The ac conductivities of the glasses were studied from 298 to 318 K and over a frequency range of 10 Hz to 10 MHz. A typical logarithmic plot of ac conductivity

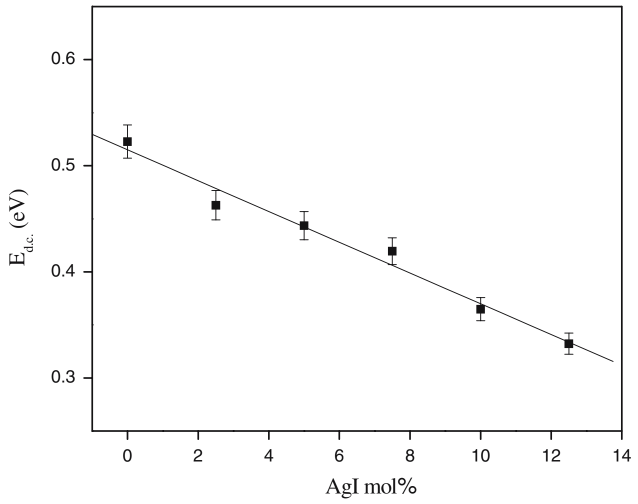

Fig. 4 Typical plot of dc activation energy (E_{dc}) versus AgI mol%

as a function of frequency for BT2 glass is shown in Fig. 5a. The ac conductivities have been fitted to Almond–West type of power law expression [49–51],

$$\sigma = \sigma_0 + A\omega^s \qquad (9)$$

where σ_0 is the dc conductivity and s is the power law exponent. The typical computer fitted conductivity data to the Eq. 9 are shown in Fig. 5b (solid lines). The behaviour of all the other glass compositions is qualitatively similar. It was found that the goodness of fit is satisfactory in all cases and hence single exponent fit seems to be adequate. The values of σ_0 obtained from the Almond–West type power law fit are similar in magnitude to the dc conductivities (σ_{dc}) obtained from the impedance plots.

The values of power law exponent s are listed in Table 2 along with the values of power law fit parameter A and goodness of fit (χ^2). The variation of power law exponent s with temperature is shown in Fig. 6. The s values are found to be almost constant and lie between 0.5 and 0.6 [52] and are essentially temperature-independent.

Dielectric relaxation behaviour

The dielectric response of the glasses has also been examined by making measurements of dielectric properties. The variation of logarithm of real (ε') and imaginary (ε'') part of dielectric constant with frequency for BT3 glass is shown in Fig. 7a and b. Since the studied glasses are highly ionic, in some cases low frequency dispersion of dielectric constant is due to the electrode polarization effects which seems to manifest at lower frequencies. As can be seen from Fig. 7a that the real part of dielectric constant seems to be flattened and it is almost temperature-independent at higher frequencies. Therefore the data has been examined using modulus representation. The variation of real

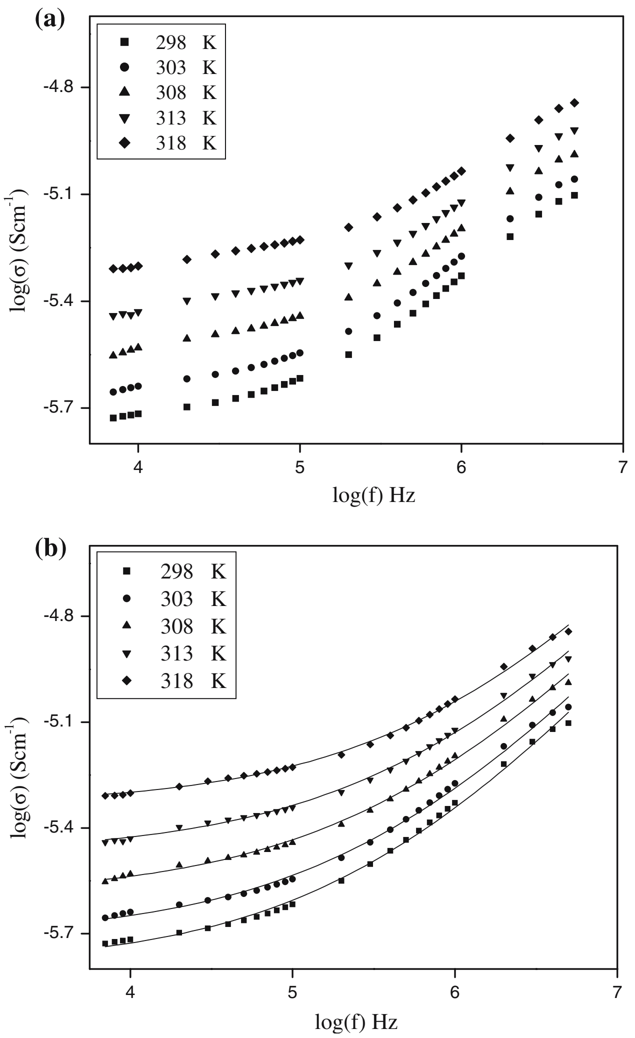

Fig. 5 Typical Plots of (**a**) log(σ) versus log(f) and (**b**) ac conductivity data fitted to single power law equation for BT2 glass at different temperatures

Table 2 Values of power law fit parameter A and the goodness of fit (χ^2) for the log(σ) versus log(f) plots at room temperature (298 K) along with s and β values

Code	A (S/cm)	s	χ^2	β
BT1	7.73×10^{-10}	0.54	0.00021	0.51
BT2	1.93×10^{-10}	0.53	0.00011	0.48
BT3	2.36×10^{-10}	0.52	0.00008	0.45
BT4	1.71×10^{-10}	0.55	0.00012	0.42
BT5	5.70×10^{-10}	0.50	0.00015	0.40
BT6	2.16×10^{-10}	0.55	0.00009	0.43

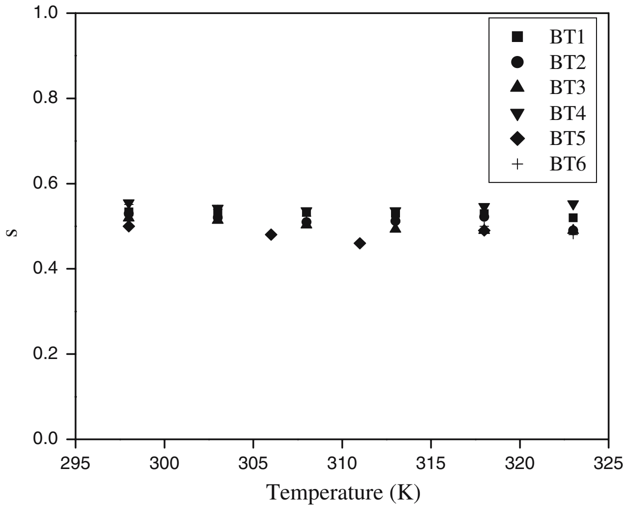

Fig. 6 Variation of power law exponent ‘*s*’ with temperature

(M') and imaginary (M'') part of dielectric modulus as a function of temperature and frequency for typical BT3 glass is shown in Fig. 8a and b. It may be also noted from Fig. 8b that the magnitude of M'' peak with temperature is found to be constant and therefore it is suggestive of the presence of single relaxation mechanism. The asymmetric and broader than Debye width of M'' originated from the nature of the relaxation behaviour and it is suggestive of stretched exponential relaxation behaviour with a characteristic β, where β is the exponent in the stretched exponential relaxation function $\phi = \phi(0)\ \exp\{-(t/\tau)^{\beta}\}$ [53–55], which is known to provide satisfactory fit for the asymmetrical M'' peaks (τ is the characteristic relaxation time). The values of β were evaluated from the full-width at half-maximum (FWHM) of M'' versus log(*f*) plots [56]. The β values are plotted as a function of temperature and it is shown in Fig. 9. The room temperature β values are listed in Table 2. The exponent β generally lies between 0 and 1, and it is widely used to describe different kinds of relaxation processes in amorphous materials. At low temperatures the relaxations occur via isolated non-interacting dipoles, becoming more and more Debye-like and β values tend towards unity [57] and there is a general tendency of β to decrease with temperature. But in the present study, the values of β seem to level off between 0.4 and 0.5 which is found to be insensitive to the variation of both temperature and composition (shown in Figs. 9, 10). If the stretched exponent β is sensitive to the variation of temperature and composition then one would have been explained its behaviour by considering an approach to treat the stretched exponential behaviour as a manifestation of a distribution of relaxation times. In the present glass system, the weak dependence of power law exponent, *s* and stretched exponent, β do not seem to relate in any simple complementary such as $s + \beta \approx 1$ [57].

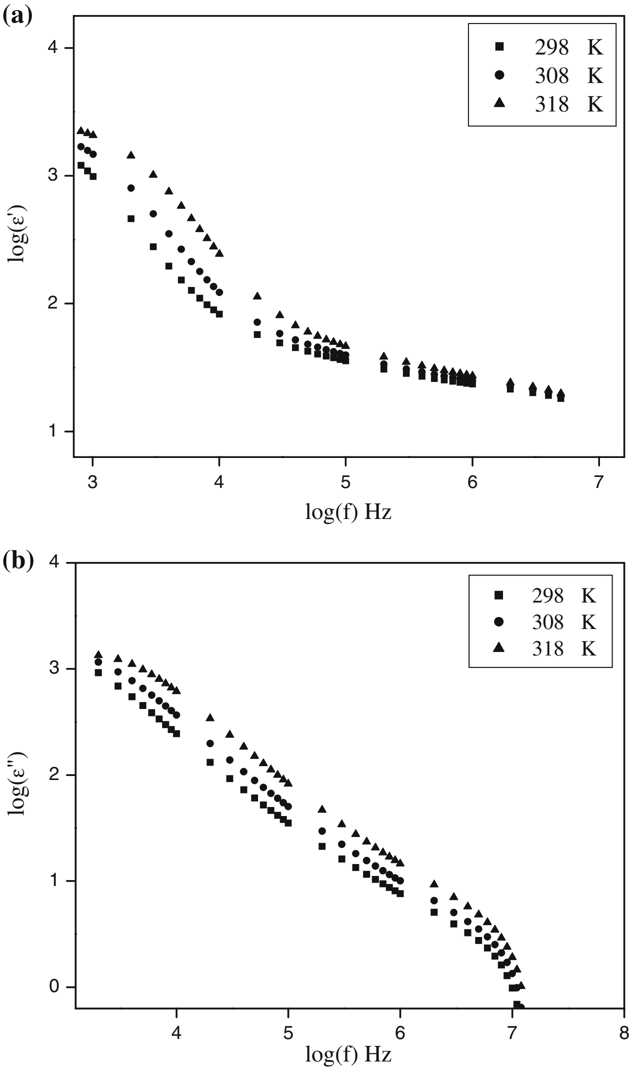

Fig. 7 Typical plots of (**a**) log(ε') and (**b**) log(ε'') versus log(*f*) for BT3 glass

The ac activation energies, E_{ac} have also been calculated from the plots of logarithmic peak frequency (in M'' versus log(*f*)) versus $1000/T$ and are given in Table 1. The variation of E_{ac} versus AgI mol% is shown in Fig. 11. E_{ac} also decreases linearly when AgI is substituted by Ag_2O. It may be also noted from Table 1 that the values of E_{ac} and E_{dc} are found to be almost similar. Thus the ac activation energies obtained from diffusion-independent (dielectric relaxation) measurements are almost same as that of the activation energies obtained from diffusion dependant (dc) conductivity measurements, suggesting a common transport mechanism in these glasses.

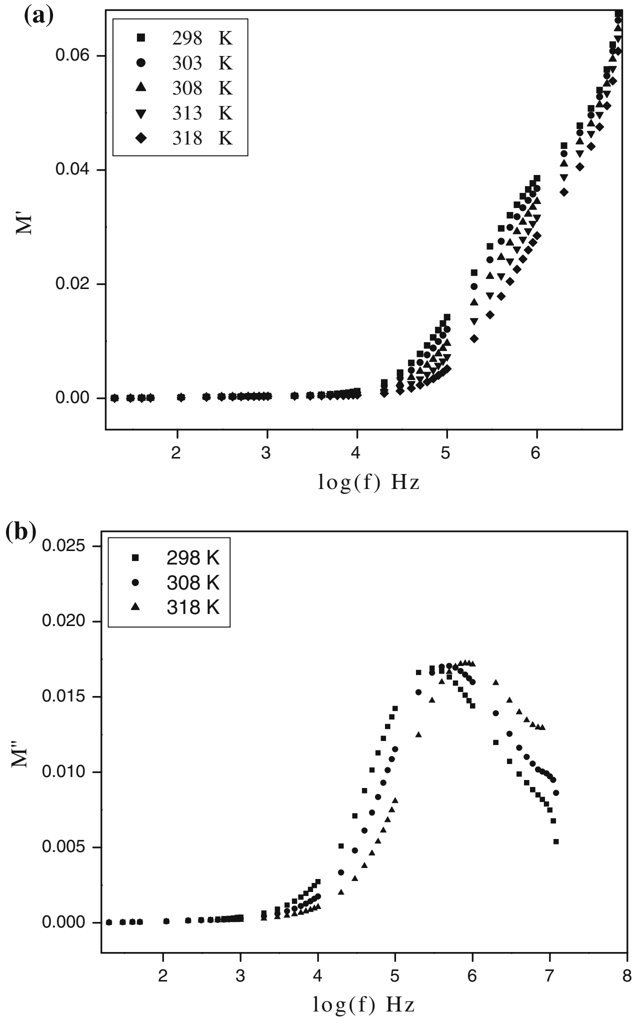

Fig. 8 Typical plots of (**a**) *M′* and (**b**) *M″* versus log(*f*) for BT3 glass

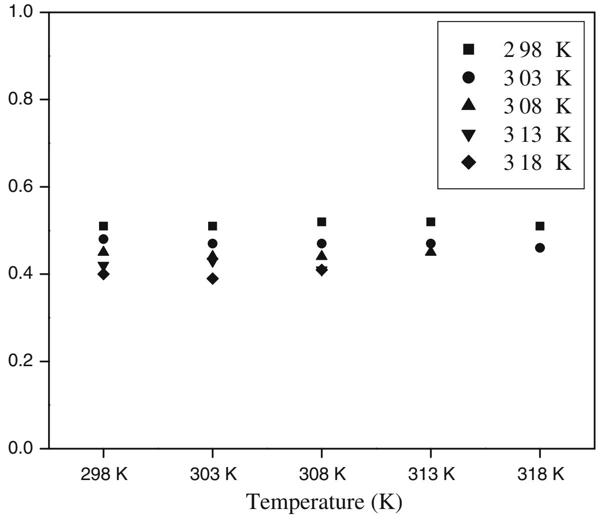

Fig. 9 Variation of stretched exponent β with temperature

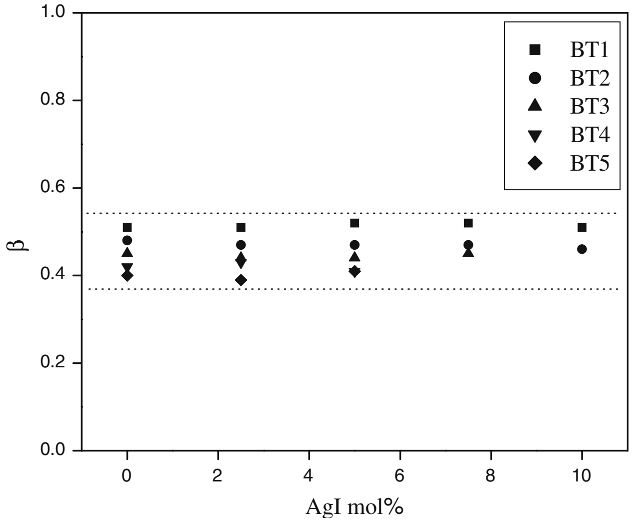

Fig. 10 Variation of stretched exponent β with composition

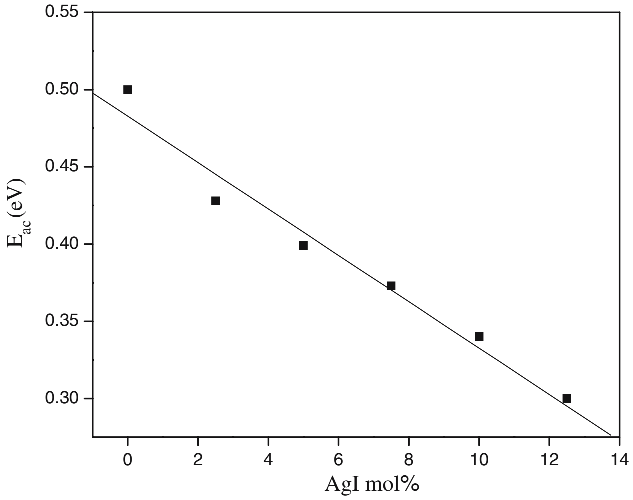

Fig. 11 Variation of E_{ac} versus AgI mol%

Reduced plots of conductivity and dielectric modulus

The reduced (master) plots of conductivity and dielectric modulus have also been studied to understand the conductivity and relaxation mechanism in silver-based boro-tellurite glasses. The reduced plots of conductivity $\log(\sigma/\sigma_0)$ and imaginary part of dielectric modulus ($M''/M''_{\max}$) versus the reduced frequency [$\log(f/f_0)$] has been plotted and it is shown in Fig. 12a and b, respectively. As can be seen from Fig. 12a and b that the plots are clearly superimposable and the data points were found to be coalesce very well for all temperatures and the different compositions studied. The superimpose of all the dielectric data on a single

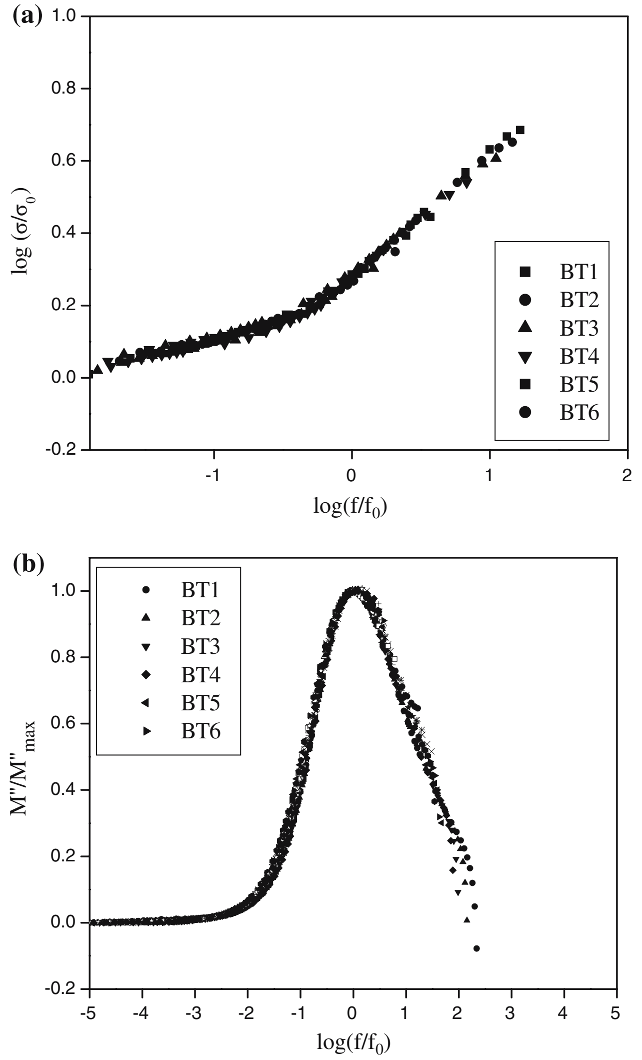

Fig. 12 Typical plots of (**a**) log(σ/σ_0) and (**b**) (M''/M''_{max}) versus log(f/f_0) for all the glasses at different temperatures

line ascertains the fact that the mechanism of ion transport is same throughout the range of temperature and compositions studied.

Conclusions

DC and AC conductivity as well as dielectric relaxation behaviour of a wide range of composition in AgI–Ag_2O–B_2O_3–TeO_2 glass system have been studied. The study of the conductivity shows that the conductivity is essentially ionic in nature and due to the Ag^+ ion motion. The dc conductivities increase with increase of AgI mol%. The ac conductivity behaviour with frequency has been fitted to Almond–West type of expression using a single exponent s. The variation of power law exponent s as a function of temperature seem to be independent. The dielectric relaxation data have been analysed using stretched exponential relaxation function. The stretched exponent β is found to be insensitive to both temperature and compositions. The superimposibility of the reduced plots of conductivity and dielectric modulus (M'') against reduced frequency clearly indicates that the ion transport mechanism is same over the wide range of temperature and compositions.

Acknowledgements The authors are grateful to Professor K.J. Rao for encouragement and many discussions. One of the authors (R.V.A) acknowledges the UGC, Govt. of India for financial support to carry out this work.

References

1. El-Damrawi G, (1994) J Non-Cryst Solids 176:91
2. Stangrennec MK, Elliott SR (1994) Solid State Ionics 73:199
3. Saunders GA, Metcalfe RD (1996) Phys Rev B 53:53
4. Ingram MD (1987) Phys Chem Glasses 28:215
5. Magistris A (1993) In: Scrosati B, Magistris A, Mari CM, and Mariatto G (eds) Proceedings of the Nato advanced research workshop on fast ion transport in solids. Kluwer Academic Publishers, Netherlands, p 213
6. El-Damrawi G, Hassan AK, Meikail MS (1996) Phys Chem Glasses 37:101
7. El-Damrawi G (1995) J Phys Condens Matter 8:1557
8. Magistris A, Chiodelli G (1983) Solid State Ionics 9 & 10:611
9. Coppo D, Duclot JJ, Souquet JL (1996) Solid State Ionics 90:111
10. Shastry MCR, Rao KJ (1989) Solid State Ionics 37:17
11. Chiodelli G, Vigano GC, Magistris A, Villa M (1983) Solid State Ionics 8:311
12. Chiodelli G, Magistris A, Villa M, Bjorkstam JL (1982) Mater Res Bull 17:1
13. Krogh-Moe J (1962) Phys Chem Glasses 3:1
14. Krogh-Moe J (1965) Phys Chem Glasses 6:46
15. Bray PJ (1996) In: Porai-Koshits E (ed) The structure of glass. Consultant Bureau, New York
16. Zhong J, Bray PJ (1989) J Non-Cryst Solids 111:67
17. Abe T (1952) J Am Ceram Soc 35:756
18. Everstein F, Stevels J, Waterman H (1960) J Phys Chem 1:123
19. Kreidl NJ (1983) In: Uhlmann DR and Kreidl NJ (eds) Glass science & technology. Academic Press, New York, p 204
20. Imaoka M, Yamazaki T (1968) J Am Ceram Soc 76:160
21. Yamamoto H, Nasu N, Mustoka J, Kanira K (1994) J Non-Cryst Solids 170:87
22. Jianrang Q, Osaka A, Tanatia T, Jakuda J, Minura Y (1992) J Mater Sci 27:3793
23. Heo J, Lam D, Sigel DH, Mendoza EA, Hensely DA (1992) J Am Ceram Soc 75:277
24. Komatsu T, Mohri H (1999) Phys Chem Glasses 40:257
25. Burger H, Kneipp K, Hobert H, Vogel W, Kozhukharov V, Neov S (1992) J Non-Cryst Solids 151:134
26. Mori H, Igarashi J, Sakata J (1995) Glasstech Ber 68:327
27. Akagi R, Handa K, Ohtori N, Hannon AC, Tatsumisago M, Umesaki N (1999) J Non-Cryst Solids 256 & 257:111
28. Sabry AI, El-Samanoudy MM (1995) J Mater Sci 30:3930
29. El-Damrawi G, Abd-El-Maksoud S (2000) Phys Chem Glasses 41(1):6

30. Kim SH, Yoko T, Sakka S (1993) J Am Ceram Soc Japan 76:2486
31. Mori H, Kitami J, Sakata H (1994) J Non-Cryst Solids 168:157
32. Rossignol S, Reau JM, Janguy B, Videau JJ, Portier J (1993) J Non-Cryst Solids 155:77
33. Jayasinghe GDLK, Coppo D, Bandaranayake PWSK, Souquet JL (1995) Solid State Ionics 76:297
34. Tatsumisago M, Minami T, Kowada Y, Adachi H (1994) Phys Chem Glasses 35:89
35. Nasu H, Matsushita O, Kamiya K, Kobayashi H, Kubodera K (1990) J Non-Cryst Solids 124:275
36. Kimura K (1989) Jpn J Appl Phys 28:810
37. Tanabe S, Hirao K, Soga N (1990) J Non-Cryst Solids 122:79
38. Lefterova ED, Angelov PV, Dimitriev YB (2000) Phys Chem Glasses 41:362
39. Jayasinghe GDLK, Bandaranayaka PWSK, Dissanayake MAKL, Gunawardane RP (1995) Solid State Ionics 78:199
40. Rodrigues ACM, Duclot MJ (1988) Solid State Ionics 28–30:729
41. Sanderson RT (1983) Polar covalence. Academic Press, New York
42. Borjessor L, Jorell LM, Howells WS (1989) Phil Mag B 59:105
43. Dalba G, Fornasini P, Fontana A, Rocca F, Burattini WS (1988) Solid State Ionics 28–30:713
44. Ratner MA, Nitzan A (1988) Solid State Ionics 28–30:3
45. Govindaraj G, Baskaran N, Shahi K, Monoravi P (1995) Solid State Ionics 76:47
46. Sebastian K, Frishat GH (1992) Phys Chem Glasses 33:199
47. Minami T, Ikeda Y, Tanaka M (1982) J Non-CrystSolids 52:159
48. Lefterova ED, Angelov PV, Dimitriev YB (2000) Phys Chem Glasses 41:362
49. Almond DP, West AR, Grant RJ (1982) Solid State Commun 44:1277
50. Almond DP, Duncan GK, West AR (1983) Solid State Ionics 8:159
51. Almond DP, Hunter CC, West AR (1984) J Mater Sci 19:3236
52. Jonscher AK (1977) Nature 267:673
53. Kohlrausch R (1847) Prog Ann 12:393
54. Williams G, Watts DC (1970) Trans Faraday Soc 66:80
55. Williams G, Watts DC, Dev SB, North AM (1971) Trans Faraday Soc 67:1323
56. Moynihan CT, Boesch LP, Laberge NL (1973) Phys Chem Glasses 14:122
57. Patel HK, Martin SW (1992) Phys Rev B 45:10292